The influence of cognitive training on brain dynamics

Guiyang Lv
Zhejiang University
Tianyong Xu
Zhejiang University
Ping Zhu
Zhejiang University
Miao Wang
Zhejiang University
Feiyan Chen
Zhejiang University
Guoguang He (gghe@zju.edu.cn)
Zhejiang University https://orcid.org/0000-0001-8031-9836

Research Article

Keywords: Brian dynamics, Functional brain networks, Abacus-based mental calculation

Posted Date: March 7th, 2022

DOI: https://doi.org/10.21203/rs.3.rs-1411610/v1

Nonlinear Dynamics manuscript No.
(will be inserted by the editor)

The influence of cognitive training on brain dynamics

Guiyang Lv · Tianyong Xu · Ping Zhu · Miao Wang · Feiyan Chen · Guoguang He*

Received: date / Accepted: date

Abstract The human brain is highly plastic. Cognitive training can make a change in functional connections between brain regions. The structures of brain networks may determine its dynamic behavior which is related to human cognitive abilities. To study the effect of functional connectivity on the brain dynamics, a dynamic model is established based on functional connectivity of the brain and the Hindmarsh-Rose model in this work. The resting-state fMRI data from the experimental group undergoing abacus-based mental calculation (AMC) training and from the control group are used to construct the functional brain networks. The local efficiency and global efficiency of the functional brain networks of the experimental group are higher than those of the control group. The dynamic behavior of brain at the resting and task states for the AMC group and the control group are simulated based on above dynamic model. In the resting state, some different activated brain regions exist between the AMC group and the control group. A stimulus with sinusoidal signals to brain networks is introduced to simulate the brain dynamics in the task states. The dynamic characteristics are extracted by the excitation rates, the response intensities and the state distributions. The change in the functional connections of brain regions with the AMC training would in turn improve the brain response to external stimulus, and make the brain more efficient in processing related tasks.

Keywords Brian dynamics · Functional brain networks · Abacus-based mental calculation

1 Introduction

The human brain is composed of billions of neurons in various levels of complex structures. Revealing the relationship between complex structures and functions of

Guiyang Lv, Tianyong Xu, Ping Zhu, Miao Wang, Feiyan Chen, Guoguang He
Department of Physics, Zhejiang University, Hangzhou, 310027, P. R. China

*Corresponding author:
G. He (E-mail: gghe@zju.edu.cn)

the brain is one of the current focuses of neuroscience. Suárez et al. built artificial neural networks with the network structures of brain regions. The networks have shown stronger performance in the memory coding task than any other network [1], which indicates that the network structure is essential for the brain to perform tasks efficiently. The work by Kanaka et al. revealed that a randomly connected recurrent neural network (RNN) can carry out memory work by modifying certain connections of the network and a signal is transmitted through the interaction between synapse and external input. It means that the neural signal sequence may emerge through learning from the unstructured network architectures [2]. Therefore, flexible and variable connections of brain regions are necessary for the brain to realize various cognitive tasks. At present, most whole-brain dynamics researches have focused on the synchronization or chimera state between brain regions by the interaction between the coupled nodes with the structural brain network [3–5]. In addition, there have been some advances in modeling neuronal dynamics [6,7]. It is lack to understand how the structures in brain networks affects the overall performance of the brain, and how the information contained in the network structures is expressed through dynamic activities.

In terms of cognitive experiments, it is known that the human brain is highly plastic [8]. Cognitive training can lead to the modification of the brain's functional excitation mode and achieve better task performance. Abacus-based mental calculation (AMC) is one of typical cognitive training method [9–11]. Previous studies have shown that the resting-state functional connections between the brain regions of the subjects would be changed by long-term abacus mental arithmetic training [12, 13]. The experiments demonstrated that AMC training can enhance the subjects' numerical processing efficiency [14] and improve their working memory [15]. Based on task-state fMRI, it was found that the brain excitation patterns and functional structures between brain regions for the experimental group with AMC training were different from those for the control group [16]. The overall performance of the brain is determined by the network structures and node dynamics [17, 18]. Up to now, most AMC researches are focused on revealing the correlation between cognitive abilities and functional structures. The influence of functional connectivity on brain dynamics is rarely reported. How functional connectivity affect the overall dynamics of the brain remains unclear.

The resting-state fMRI data of the AMC group and the control group are collected to establish the functional networks and dynamic behaviors of functional networks from the AMC group and the control group are investigated in this work. Considering that the Hindmarsh-Rose (HR) model has a wealth of dynamic characteristics from neurons to neuron clusters [19], the HR model is used as a node to replace one brain region in the network. In this way, a complete brain dynamics model is therefore constructed. Our previous work has proved that this model can well simulate the dynamic behavior of the brain at resting-state [20]. Using this model, we try to study the dynamic differences between the AMC group and the control group and reveal the functions of AMC training on brain dynamics.

The rest of this article is structured as follows. The resting-state functional brain networks are introduced in the second section and the comparison of functional brain networks between the AMC group and the control group is made. In the third section, the resting-state brain network dynamics model is described and simulations are conducted. The task-state brain dynamics model is given in

the fourth section and the dynamic differences between the AMC group and the control group are pointed out too. The conclusion is arranged in the last section.

2 Functional brain network of the resting-state

The structures of functional networks in the resting-state are similar to those in the task-induced states to some extent [21,22], and the task-related activation patterns can be explained partly by the functional connections between brain regions in the resting-state [23]. In order to study the effect of functional connectivity on brain dynamics, we collect fMRI data of 25 subjects trained by AMC and other 25 subjects as a control group. The data are measured in the resting-state. The corresponding functional networks in the resting-state are constructed. All subjects are from urban families, have normal hearing, normal or corrected vision, no neurological or mental disorders, and no special educational assistance requirements. Participants in the experimental group and the control group are randomly selected. The details about the experiment can be found in the reference [24].

The AAL template is used to divide the whole brain into 90 brain regions, as shown in Table 1. The correlations between brain regions are expressed by Pearson correlation. The correlation coefficient matrix of the functional brain network for a subject is denoted by R. R_{ij} is the correlation coefficient between the i-th and j-th brain regions. After averaging the functional connection matrices of the AMC group and the control group, two corresponding correlation coefficient matrices are obtained. The correlation coefficient matrices are shown in Fig. 1. We found that the AMC group show higher correlation coefficients between brain regions, which means the correlations between brain regions for the AMC group are closer than those for the control group.

Table 1 Regions of interest included in the AAL-atlas (45 in each cerebral hemisphere, 90 in total, odd/even numerical order for left/right hemisphere)

Number	Full name	Abbreviation	Number	Full name	Abbreviation
1,2	Precentralgyrus	PreCG	47,48	Lingualgyrus	LING
3,4	Superiorfrontalgyrus(dorsal)	SFGdor	49,50	Superioroccipitalgyrus	SOG
5,6	Orbitofrontalcortex(superior)	ORBsup	51,52	Middleoccipitalgyrus	MOG
7,8	Middlefrontalgyrus	MFG	53,54	Inferioroccipitalgyrus	IOG
9,10	Orbitofrontalcortex(middle)	ORBmid	55,56	Fusiformgyrus	FFG
11,12	Inferiorfrontalgyrus(opercular)	IFGoperc	57,58	Postcentralgyrus	PoCG
13,14	Inferiorfrontalgyrus(triangular)	IFGtriang	59,60	Superiorparietalgyrus	SPG
15,16	Orbitofrontalcortex(inferior)	ORBinf	61,62	Inferiorparietallobule	IPL
17,18	Rolandicoperculum	ROL	63,64	Supramarginalgyrus	SMG
19,20	Supplementarymotorarea	SMA	65,66	Angulargyrus	ANG
21,22	Olfactory	OLF	67,68	Precuneus	PCUN
23,24	Superiorfrontalgyrus(medial)	SFGmed	69,70	Paracentrallobule	PCL
25,26	Superiorfrontalcortex(medialorbital)	ORBsupmed	71,72	Caudate	CAU
27,28	Rectusgyrus	REC	73,74	Putamen	PUT
29,30	Insula	INS	75,76	Pallidum	PAL
31,32	Anteriorcingulategyrus	ACG	77,78	Thalamus	THA
33,34	Mediancingulategyrus	DCG	79,80	Heschlgyrus	HES
35,36	Posteriorcingulategyrus	PCG	81,82	Superiortemporalgyrus	STG
37,38	Hippocampus	HIP	83,84	Temporalpole(superior)	TPOsup
39,40	Parahippocampalgyrus	PHG	85,86	Middletemporalgyrus	MTG
41,42	Amygdala	AMYG	87,88	Temporalpole(middle)	TPOmid
43,44	Calcarinecortex	CAL	89,90	Inferiortemporalgyrus	ITG
45,46	Cuneus	CUN			

The clustering coefficient C and the characteristic path length L are used to analyze the properties of the functional networks. The clustering coefficient C is defined as the ratio of the actual number of connections between all nodes to the number of all possible connections, which characterizes the local efficiency of a network. The characteristic path length L is defined as $L = \frac{1}{N(N-1)} \sum_{i \neq j} l_{ij}$, where N is the number of nodes in a network, and l_{ij} is the shortest path connecting the

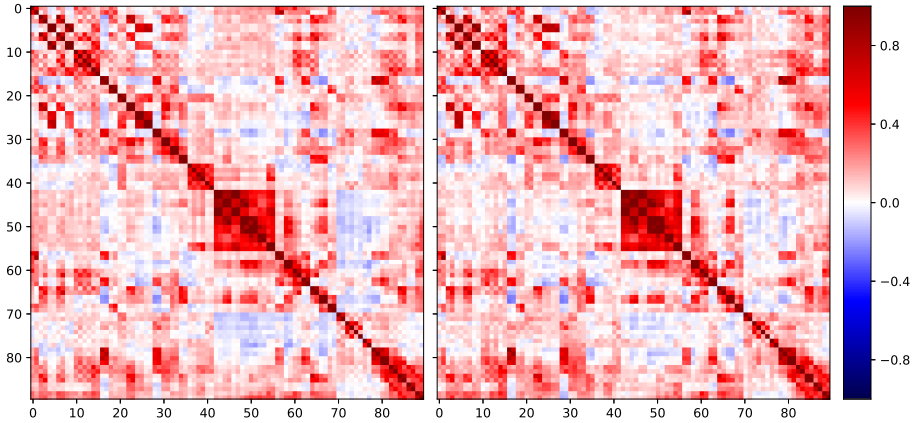

Fig. 1 Correlation coefficient matrices of the control group and AMC group. The left picture is the control group, and the right one is the AMC group.

i-th node and the j-th node. The smaller the characteristic path length L is, the higher the overall efficiency of the network become. In addition, in constructing a functional brain network, experimental noise should be removed while the connection density between brain regions is in a reasonable range to ensure there are no isolated nodes. It is therefore necessary to select a threshold T for the correlation coefficient matrix. When the absolute value of the correlation coefficient R_{ij} is less than T, it is considered that there is no functional connection between the two brain regions, and the R_{ij} is turned to be 0. C and L of the brain networks for both the experimental group and the control group are calculated at different thresholds, as shown in Fig. 2.

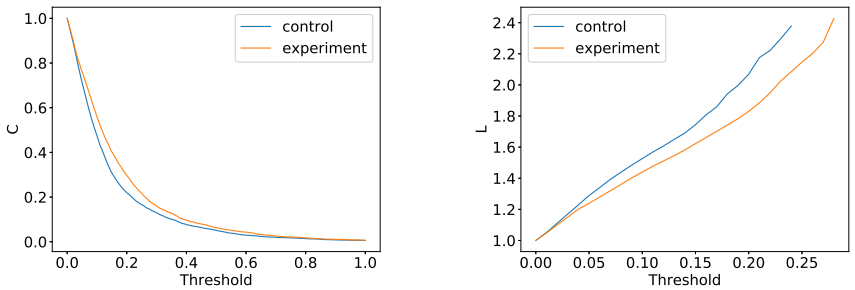

(a) (b)

Fig. 2 (a) Clustering coefficients of brain networks under different thresholds. (b) The characteristic path length of the brain network under different thresholds.

Compared with the control group, the clustering coefficient C of the AMC group is larger at different T, which means the AMC group has higher local efficiency, as shown in Fig. 2(a). Meanwhile, the L of the AMC group is shorter than that of the control group, which means the information transmission efficiency of

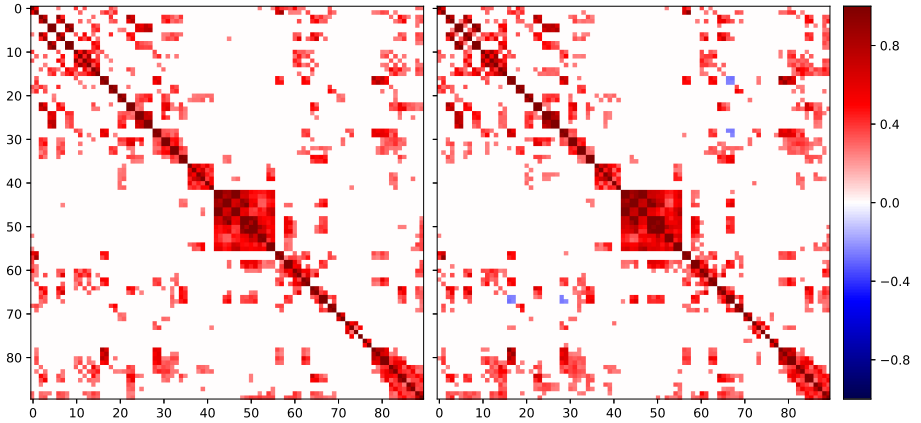

Fig. 3 The correlation coefficient matrices of the control group and the experimental group after threshold processing. The left picture is the control group, and the right one is the AMC group

the AMC group is higher. It is demanded that information should be transmitted over whole networks in the calculation of the shortest path. Therefore, the calculation of the shortest path is ended when any isolated cluster appears. The cut-off threshold of the experimental group is higher than that of the control group, as shown in Fig. 2(b), which indicates that AMC training can improve the overall and partial efficiency and the robustness of the brain network.

Based on the above results, we obtain the weight matrix W by setting the network threshold T to 0.24, as shown in Fig. 3. It is found that the connections between brain regions of the AMC group look similar to that of the control group, but the connection density and connection strength of the AMC group are higher than that of the control group, which means the correlations between brain regions are stronger for AMC group.

3 Resting-state brain dynamics

3.1 Model of resting-state brain dynamics

HR model contains most dynamic properties observed at the level of real neurons, such as regular and irregular spiking and bursting, and at the level of the collective brain dynamics. In order to explore the influence of functional connections between brain regions on the dynamic activities of the brain, HR model is introduced to functional brain networks of the AMC group and the control group. A dynamics model for a resting-state functional brain network is established by using the HR model instead of brain regions and the correlation coefficients between brain regions as the connection weights. The dynamics model is described by the following equations.

$$\begin{aligned}
\dot{x}_i &= y_i - ax_i^3 + bx_i^2 - z_i + I_{bias} + \frac{\sigma}{90}\sum_{j=1}^{90} W_{ij}x_j \\
\dot{y}_i &= c - dx_i^2 - y_i + \frac{\sigma}{90}\sum_{j=1}^{90} W_{ij}y_j \\
\dot{z}_i &= r\left[s(x_i - x_r) - z_i\right] \\
W_{ij} &= \begin{cases} R_{ij} & ,if\ |R_{ij}| \geq T \\ 0 & ,otherwise \end{cases}
\end{aligned} \quad , \tag{1}$$

where x_i represents the output signal of the i-th brain region, and a, b, c, d, r, s, and x_r are model parameters. I_{bias} is the bias current, which regulates the intensity of dynamic activity of brain regions. σ is the gain coefficient, which regulates the connection strength between brain regions. These parameters are set as follows, $a = 1.0$, $b = 3.0$, $c = 1.0$, $d = 5.0$, $s = 4.0$, $r = 0.006$, $x_r = -1.56$, $I_{bias} = 1.6$, $\sigma = 1.2$. We find that all brain regions in the functional brain networks of the AMC group and the control group exhibit bursts of spikes, as shown in Fig. 4(a). Different from a single HR model, the nodes in the networks show obvious entrainment behaviors, that is, the fast oscillations of the encoded signals is mixed with lower frequency oscillations, which is an effective means for information transmission between neurons [25, 26]. The dynamic behaviors shown in Fig. 4(a) are consistent with the remote communication mode in the brain, in which low-frequency resonances determine the long-distance information exchange while high-frequency oscillations characterizes the local neural activity in the brain [27].

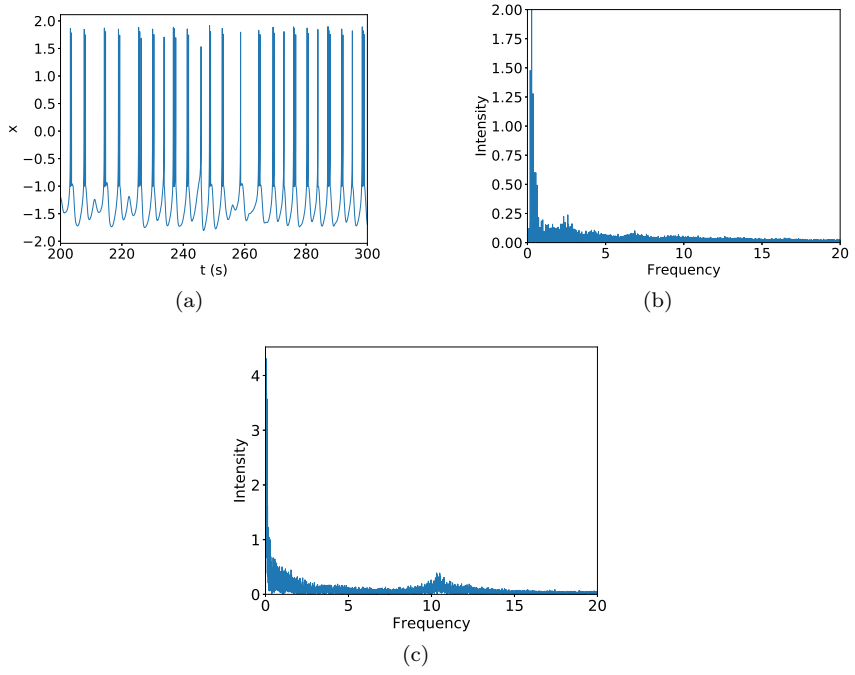

Fig. 4 (a)The signal of PUT(R) of control group. (b) Spectrum distribution of PUT (R)'s signal. (c) Typical resting-state EEG spectrum distribution.

We perform Fourier transform on the output signals of brain regions. Fourier transform of Fig. 4(a) is shown in Fig. 4(b). Compared with the resting state EEG signal shown in Fig. 4(c), it can be found that the spectrum characteristics of the output signals generated by our model is consistent with that of the resting state EEG signals.

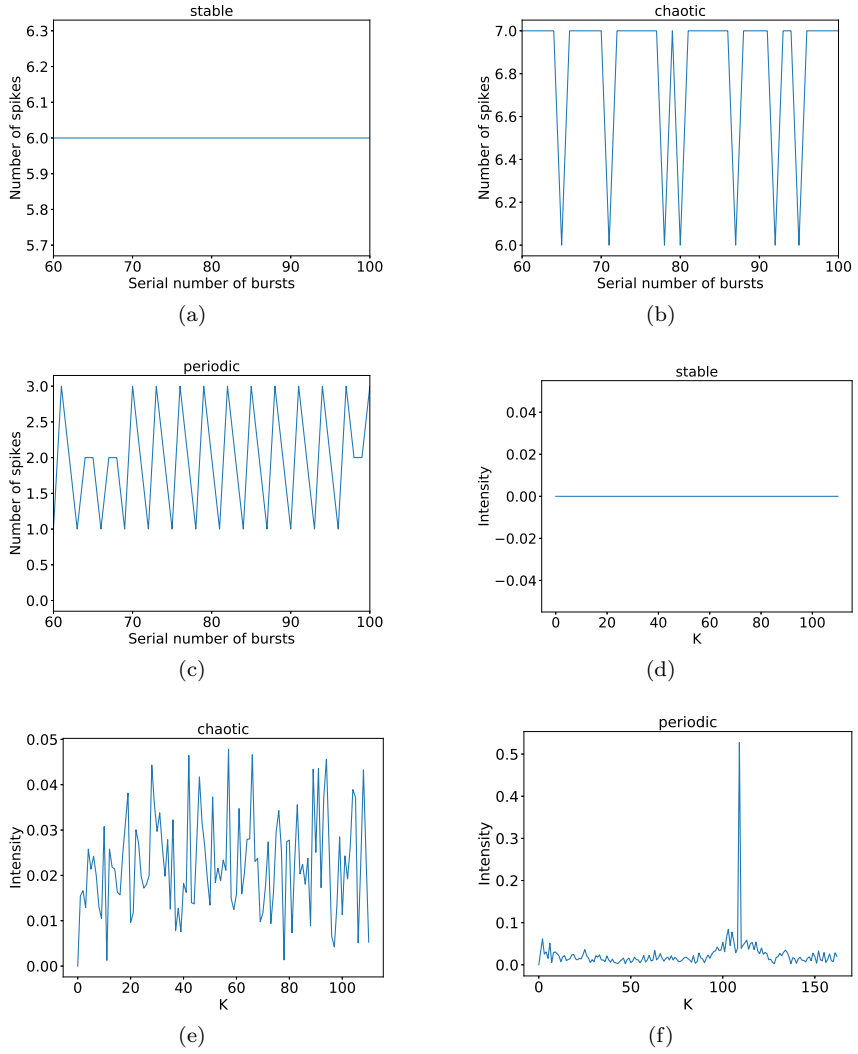

Fig. 5 The numbers of spikes and their spatial transformations of different modes (control group). (a, d) IFGoperc(L), stable mode. (b, e) TPOsup(R), chaotic mode. (c, f) PUT(R), periodic mode.

In order to analyze the dynamic characteristics of brain regions, we count the spikes in bursts. The spikes in bursts are almost stable or random in some

brain regions, while in other brain regions spikes in bursts looks similar periodic, as shown in Fig. 5(a)-5(c). In order to distinguish the dynamic behavior of the brain regions, we make spatial transformation on the spikes according to Eq. 2. M_n represents the number of spikes in the n-th burst, and N represents the total number of bursts. The results of spatial transformation on the spikes are shown in Fig. 5(d)-5(f). The dynamic behaviors of brain regions can be divided into the stable mode, the chaotic mode, and the periodic mode.

$$F(\mathbf{k}) = \left| \sum_{n=0}^{N-1} M_n e^{-i2\pi kn/N} \right| /N \tag{2}$$

3.2 The resting-state dynamics between the AMC group and control group.

Our previous work has revealed that the brain regions in periodic mode are active ones [20]. Under the same parameter settings, we obtain all activated brain regions of the AMC group and the control group under the same parameter settings. As shown in Fig. 6, the AMC group and the control group have some common activated brain regions under the same parameter settings, namely CAU(R) and PUT(L, R) brain areas. CAU and PUT form the basal ganglia, which play an important role in advanced cognitive activities such as learning, memory, reward, motivation, emotion, and romantic interaction [28, 29]. Meanwhile, different activated brain regions exist between the AMC group and the control group. For example, OLF(R), PHG(L), and THA(R) are activated only in the AMC group, while CAU(L) brain region is activated in the control group. More brain regions are inspired in the AMC group. It is confirmed that AMC training induces functional changes in brain activation and such plasticity may be transferable beyond the AMC [30].

For the AMC group and the control group, functional brain networks are a bit different in the resting state. Our dynamical simulations based on the resting-state functional brain network prove the differences of brain activation between the AMC group and the control group since the different connections of functional brain networks.

(a) (b)

Fig. 6 (a)Activated brain area of control group. (b) Activated brain area of AMC group. The figure is plotted with BrainNet Viewer [31].

4 Task state brain dynamics

4.1 Dynamic characteristics of task states

We add sinusoidal signals to brain networks to simulate the brain dynamics in the task states. The dynamic model of the brain is transferred as follows.

$$\begin{aligned} \dot{x}_i &= y_i - ax_i^3 + bx_i^2 - z_i + I_{bias} + I_{ext} + \frac{\sigma}{90}\sum_{j=1}^{90} W_{ij}x_j \\ \dot{y}_i &= c - dx_i^2 - y_i + \frac{\sigma}{90}\sum_{j=1}^{90} W_{ij}y_j \\ \dot{z}_i &= r\left[s(x_i - x_r) - z_i\right] \\ I_{ext} &= 48 \times \sin(2\pi \times t/cycle) \end{aligned} \quad , \tag{3}$$

I_{ext} is an external sine stimulus, and the other parameters are the same as those used in section 3. After adding the sinusoidal signals, the activities of most brain regions become periodic mode. The result further demonstrates that the periodic mode is a kind of active performance. We count the excitation rate (the proportion of brain regions in the periodic mode) and the response intensity (the average dynamic intensity of brain regions obtained under Fourier transform at the same cycle as the external sinusoidal signals). The response intensity represents the synchronization of networks.

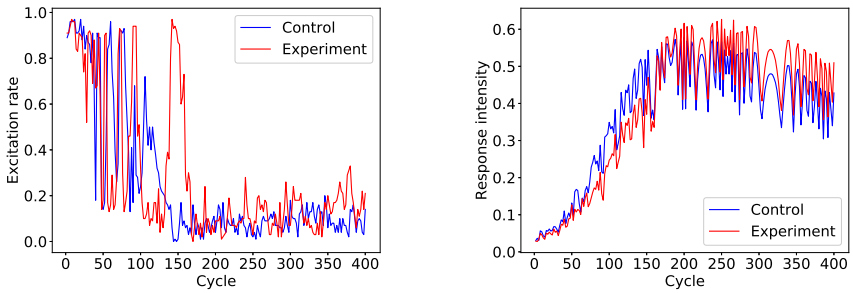

(a) (b)

Fig. 7 (a) The excitation rates. (b) The average response intensities.

As shown in Fig. 7(a), when the cycle of the sinusoidal signals is near 150 (the time length in the HR model), the dynamics of the brain networks varies significantly. At small cycle, the excitation rates of the AMC group and the control group are similar, and both show high excitation rates. When the cycle is about 150 or above 150, the periodic mode is suppressed, and the AMC group exhibits a higher excitation rate than the control group. The response intensities at different cycles are plotted in Fig. 7(b). The response intensity is dependent on the cycle. When the cycle is less than 150, the response intensity displays positive correlation with the cycle, and the response intensity of the AMC group is lower than that of the control group. When the cycle is greater than 150, the response intensities of the two groups are relatively stable, while the response intensity of the AMC is higher than that of the control group.

4.2 State space analysis

The state space is a two-dimensional space shaped by the average time width of the bursts and the average number of spikes in the bursts, and is used to describe the communication behavior between the neuron clusters [25]. We introduce the state space to find out the origin of the dynamic differences between the AMC group and the control group. We mark the dynamic behaviors of all brain regions for the AMC group and the control group with the stimulus of sinusoidal signals at different cycles in the state space, as shown in Fig. 8.

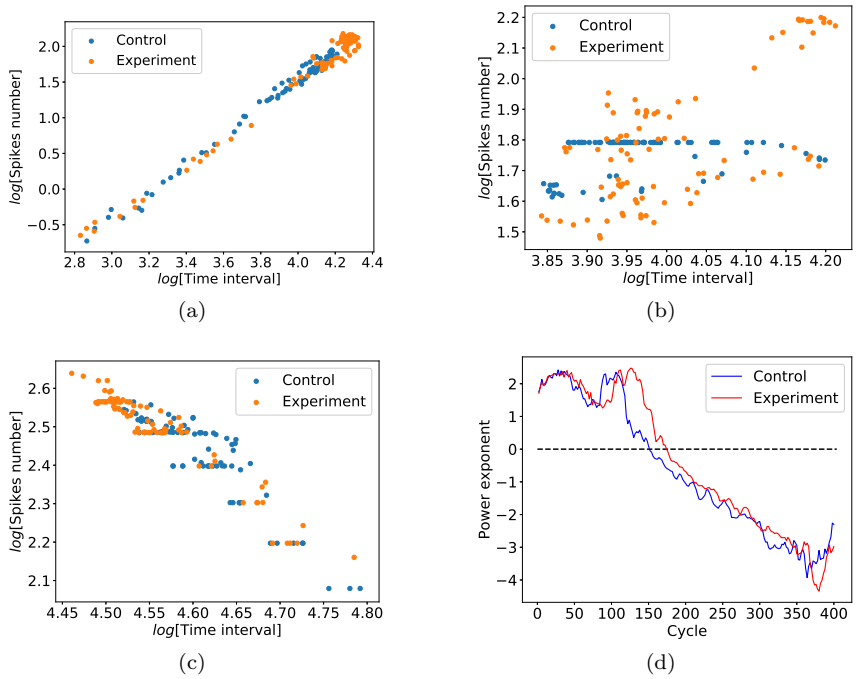

Fig. 8 The distributions of brain activities in the state space with the stimulus of sinusoidal signals at different cycles. (a)Cycle = 8. (b) Cycle = 144. (c) Cycle = 256. (d) Power exponents.

Analyzing the distributions of brain region activities in the state space, it is observed that obvious mode switching exists for both groups as the cycle of sinusoidal signals increases, as shown in Fig. 8(a)-8(c). In the state space, the power exponents of the state distributions of the brain activities evolve from positive to negative as the cycle of sinusoidal signals increases. The power law is direct evidence that the brain works near a critical state [32, 33]. Near the transition points between positive and negative exponents, the average excitation rates of both groups decrease rapidly as shown in Fig. 7(a). The response intensity represents the synchronization of networks. From Fig. 7(b), one can find that the overall synchronization of the brain networks for both groups has positive correlation with the cycle below the transition points and reach the maximum near the

transition points. We define the states of brain networks with a high excitation rate and positive power exponent as the overall task states, and others are the critical state with high synchronous oscillation.

As shown in Fig. 7, the AMC group has a higher excitation rate, but a lower response intensity during the overall task states than the control group, which means that the AMC group can do tasks with less concussion and higher efficiency by integrating the functional brain networks. The difference of the power exponents between the AMC group and the control group shown in Fig. 8(d) indicates that the AMC group exhibits the overall task states in longer length of cycles, that is, the AMC group has stronger ability to perform task. In addition, the power exponents with different cycles also show a power law, which indicates further that the brain works near the critical state.

Previous research has shown that AMC training can lead to a change in the excitation patterns of the subjects' brain [11,13], strengthen working memory [15], and improve the efficiency of numerical processing [14, 34]. Evidence shows that these changes may be transferable beyond the AMC [30]. Our simulations based on functional brain networks confirm the differences of brain dynamics between the AMC group and control group, and AMC training can enhance the abilities of subjects to perform tasks. Since we use the same models for the AMC group and control group, our results indicate that the differences of brain dynamics come from the change of functional structures in brain networks by AMC training.

5 Conclusion

Study on the topological structures of functional brain networks proves that AMC training can change the structure of functional brain networks of the subjects, making the networks have higher local and global efficiency. The dynamic behavior of brain at the resting and task states for the AMC group and the control group are simulated with the dynamic model established based on functional brain networks and HR model. For the resting state, besides the common activated brain regions, some different activated brain regions exist between the AMC group and the control group. A stimulus with sinusoidal signals to brain networks is used to simulate the brain dynamics in the task states. The dynamic characteristics are extracted by the excitation rates, the response intensities and the state distributions. Observing these quantities at different cycles of sinusoidal signals, obvious mode switching exists near the cycle of 150 for both groups. The state distributions of brain in the state space are expressed as a power law. The power exponents are dependent on the cycle of the external signals and turn from positive power exponent to negative ones as the cycle of the external signals increases. The transition points are near the cycle of 150. It is confirmed that brain works near a critical state. Compared with the control group, the AMC group has a higher excitation rate, but a lower response intensity below the cycle of 150 at the stimulus of sinusoidal signals and the AMC group has a longer active period of the overall task states, which indicates that the AMC group have stronger abilities to do tasks.

Our work proves that the changes in the functional structures of the brain with AMC training make the dynamic behaviors of subjects more efficient. The research method proposed in this work can be used to simulate the dynamic behavior of the brain and evaluate its dynamic performance.

Acknowledgements This work was supported by the Natural Science Foundation of China (Grant no.31270026).

Compliance with ethical standards

Ethics Statement

This study was approved by the research ethics review board of Zhejiang University in China, and was conducted in accordance with the guidelines of Helsinki Declaration. All children and their parents were provided informed written consent and signed it before the experiment. We acquired signed written consent to publish their MRI images.

Conflict of interest

The authors declare that they have no conflict of interest.

Data and code availability statement

Considering that data of this study are still analyzed for further research, we cannot share the data publicly at the moment. Data are only available from the Bio-X Laboratory, Department of Physics, Zhejiang University, Hangzhou, China. Interested researchers should contact Dr. Feiyan Chen by e-mail chenfy@zju.edu.cn.

References

1. L.E. Suárez, B.A. Richards, G. Lajoie, B. Misic, Nature Machine Intelligence **3**(9), 771 (2021)
2. K. Rajan, C.D. Harvey, D.W. Tank, Neuron **90**(1), 128 (2016)
3. A. Haimovici, E. Tagliazucchi, P. Balenzuela, D.R. Chialvo, Physical review letters **110**(17), 178101 (2013)
4. M. Breakspear, Nature neuroscience **20**(3), 340 (2017)
5. M.L. Kringelbach, J. Cruzat, J. Cabral, G.M. Knudsen, R. Carhart-Harris, P.C. Whybrow, N.K. Logothetis, G. Deco, Proceedings of the National Academy of Sciences **117**(17), 9566 (2020)
6. Y. Xu, Y. Guo, G. Ren, J. Ma, Applied Mathematics and Computation **385**, 125427 (2020)
7. Y. Xu, M. Liu, Z. Zhu, J. Ma, Chinese Physics B **29**(9), 098704 (2020)
8. B. Kolb, I.Q. Whishaw, Annual review of psychology **49**(1), 43 (1998)
9. F. Du, F. Chen, Y. Li, Y. Hu, M. Tian, H. Zhang, BioMed Research International **2013** (2013)
10. Y. Li, F. Chen, W. Huang, Neural Plasticity **2016** (2016)
11. Y. Xie, J. Weng, C. Wang, T. Xu, X. Peng, F. Chen, Neuroimage **183**, 811 (2018)
12. Y. Li, Y. Hu, M. Zhao, Y. Wang, J. Huang, F. Chen, Brain research **1539**, 24 (2013)
13. H. Zhou, F. Geng, T. Wang, C. Wang, Y. Xie, Y. Hu, F. Chen, Neuroscience **432**, 115 (2020)
14. Y. Yao, F. Du, C. Wang, Y. Liu, J. Weng, F. Chen, Frontiers in human neuroscience **9**, 245 (2015)
15. S. Dong, C. Wang, Y. Xie, Y. Hu, J. Weng, F. Chen, Neuroscience **332**, 181 (2016)
16. F. Chen, Z. Hu, X. Zhao, R. Wang, Z. Yang, X. Wang, X. Tang, Neuroscience letters **403**(1-2), 46 (2006)

17. L. Büsing, B. Schrauwen, R. Legenstein, Neural computation **22**(5), 1272 (2010)
18. F. Mastrogiuseppe, S. Ostojic, Neuron **99**(3), 609 (2018)
19. C. Siettos, J. Starke, Wiley Interdisciplinary Reviews: Systems Biology and Medicine **8**(5), 438 (2016)
20. G. Lv, N. Zhang, K. Ma, J. Weng, P. Zhu, F. Chen, G. He, Nonlinear Dynamics **104**(2), 1475 (2021)
21. M.D. Greicius, V. Menon, Journal of cognitive neuroscience **16**(9), 1484 (2004)
22. S.M. Smith, P.T. Fox, K.L. Miller, D.C. Glahn, P.M. Fox, C.E. Mackay, N. Filippini, K.E. Watkins, R. Toro, A.R. Laird, et al., Proceedings of the national academy of sciences **106**(31), 13040 (2009)
23. M. Mennes, C. Kelly, X.N. Zuo, A. Di Martino, B.B. Biswal, F.X. Castellanos, M.P. Milham, Neuroimage **50**(4), 1690 (2010)
24. C. Wang, T. Xu, F. Geng, Y. Hu, Y. Wang, H. Liu, F. Chen, Journal of Neuroscience **39**(33), 6439 (2019)
25. G. Hahn, A. Ponce-Alvarez, G. Deco, A. Aertsen, A. Kumar, Nature Reviews Neuroscience **20**(2), 117 (2019)
26. E. Florin, S. Baillet, Neuroimage **111**, 26 (2015)
27. G. Buzsaki, A. Draguhn, science **304**(5679), 1926 (2004)
28. M.E. Driscoll, P.C. Bollu, P. Tadi, StatPearls [Internet] (2020)
29. M. Ghandili, S. Munakomi, StatPearls [Internet] (2021)
30. H. Zhou, F. Geng, Y. Wang, C. Wang, Y. Hu, F. Chen, Neuroscience **408**, 135 (2019)
31. M. Xia, J. Wang, Y. He, PloS one **8**(7), e68910 (2013)
32. A.J. Fontenele, N.A. de Vasconcelos, T. Feliciano, L.A. Aguiar, C. Soares-Cunha, B. Coimbra, L. Dalla Porta, S. Ribeiro, A.J. Rodrigues, N. Sousa, et al., Physical review letters **122**(20), 208101 (2019)
33. L.J. Fosque, R.V. Williams-García, J.M. Beggs, G. Ortiz, Physical Review Letters **126**(9), 098101 (2021)
34. Y. Wang, F. Geng, Y. Hu, F. Du, F. Chen, Cognition **127**(2), 149 (2013)